

Numerical turbulence simulations of intermittent fluctuations in the scrape-off layer of magnetized plasmas

G. Decristoforo,^{a)} A. Theodorsen,^{a)} J. Omotani,^{b)} T. Nicholas,^{c)} and O. E. Garcia^{a)}

(Dated: 16 February 2021)

Intermittent fluctuations in the boundary of magnetically confined plasmas are investigated by numerical turbulence simulations of a reduced fluid model describing the evolution of the plasma density and electric drift vorticity in the two-dimensional plane perpendicular to the magnetic field. Two different cases are considered, one describing resistive drift waves in the edge region and another including only the interchange instability due to unfavorable magnetic field curvature in the scrape-off layer. Analysis of long data time series obtained by single-point recordings are compared to predictions of a stochastic model describing the plasma fluctuations as a super-position of uncorrelated pulses. For both cases investigated, the radial particle density profile in the scrape-off layer is exponential with a radially constant scale length. The probability density function for the particle density fluctuations in the far scrape-off layer has an exponential tail. Radial motion of blob-like structures leads to large-amplitude bursts with an exponential distribution of peak amplitudes and the waiting times between them. The average burst shape is well described by a two-sided exponential function. The frequency power spectral density of the particle density is simply that of the average burst shape and is the same for all radial positions in the scrape-off layer. The fluctuation statistics obtained from the numerical simulations are in excellent agreement with recent experimental measurements on magnetically confined plasmas. The statistical framework defines a new validation metric for boundary turbulence simulations.

^{a)}Department of Physics and Technology, UiT The Arctic University of Norway, NO-9037 Tromsø, Norway

^{b)}United Kingdom Atomic Energy Authority, Culham Centre for Fusion Energy, Culham Science Centre, Abingdon, Oxon, OX14 3DB, UK

^{c)}York Plasma Institute, Department of Physics, University of York, Heslington, York YO10 5DD, UK

I. INTRODUCTION

At the boundary of magnetically confined plasma, turbulent transport of particles and heat in the outermost region enhances plasma interactions with the material surfaces. This can become a serious issue for future fusion experiments and reactors.¹⁻³ A complete description of the physical mechanisms underlying the cross-field plasma and heat transport in the scrape-off layer (SOL) and its effects on plasma-wall interactions is necessary if reliable predictions for reactor relevant devices are to be obtained. Unfortunately, such an understanding is at present still not fully achieved and predictions and extrapolations are often based on empirical scaling laws or highly simplified transport modelling with limited theoretical foundation.³⁻⁵

Fluctuations and turbulent motions in the boundary region of magnetized plasmas have been extensively investigated both experimentally and theoretically. It is recognized that in the SOL radial motion of blob-like filament structures is the dominant mechanism for cross-field transport of particles and heat.⁶⁻⁹ This leads to broadening and flattening of radial profiles and high average particle density in the SOL that increases plasma-wall interactions.¹⁰⁻²³ Experimental measurements using Langmuir probes and gas puff imaging have revealed highly intermittent fluctuations of the particle density in the far SOL. Interestingly, measurements across a variety of magnetic geometries, including conventional tokamaks, spherical tokamaks, reversed field pinches and stellarators have shown similar fluctuation characteristics.²⁴⁻²⁷ Recent statistical analysis of exceptionally long fluctuation data time series from several tokamak devices has shown that the fluctuations are well described as a super-position of uncorrelated exponential pulses with fixed duration, arriving according to a Poisson process and with exponentially distributed pulse amplitudes.²⁸⁻⁴² A statistical framework based on filtered Poisson processes has proven an accurate description of both average radial profiles and fluctuations in the boundary of magnetically confined plasma.⁴³⁻⁵³

So far, this stochastic model has not been utilized to analyze fluctuation data from numerical turbulence simulations of the boundary region of magnetized plasmas. In order to obtain statistically significant results, long simulation data time series or a large ensemble are required, equivalent to several hundred milliseconds in experiments with medium-sized magnetically confined plasma. Since most turbulence simulation studies have been focused on the dynamics of individual blob structures or on the effects of specific physical mechanisms on turbulence and transport, the simulations have likely not produced time series data of sufficient duration in order to analyze them in the same manner as the experimental measurements.²⁸⁻⁴² In this paper we present the first

results from applying the same statistical framework on numerical simulation data as has recently been done on experimental measurements. By using a simplified turbulence model describing the fluctuations in the two-dimensional plane perpendicular to the magnetic field, we have obtained data time series sufficiently long to allow unambiguous identification of the fluctuation statistics. The main goal of this study is to clarify these statistical properties and compare them with that found from experimental measurements. This is considered an essential step towards validation of turbulence simulation codes.^{54–56}

A recent analysis of fluctuation data time series obtained from numerical simulations of turbulent Rayleigh–Bénard-convection in two dimensions has given some illuminating results.⁵⁷ This model has frequently been used as a simplified description of the non-linear interchange dynamics in the SOL of magnetically confined plasmas.^{58–66} In Ref. 57 it was found that the fluctuation time series are well described as a super-position of Lorentzian pulses, resulting in an exponential frequency power spectral density. In the present study, more sophisticated models for SOL turbulence are investigated, including sheath dissipation due to losses along magnetic field lines intersecting material surfaces as well as drift wave dynamics in the edge region.^{67–83} The resulting far SOL data time series are shown to be dominated by large-amplitude bursts with a two-sided exponential pulse shape and fluctuation statistics that compare favorably with those found in experimental measurements.^{28–42}

In this contribution we present a detailed statistical analysis of fluctuation data time series from numerical simulations of a two-dimensional reduced fluid model describing the evolution of the electron density and electric drift vorticity. The paper is structured as follows. The reduced fluid model equations, normalization and parameters are discussed in Sec. II. A brief introduction to the stochastic model is also presented here. We present the results for the time-averaged profiles and probability densities in Sec. III and for the fluctuation statistics in Sec. IV. A discussion of the results and the conclusions are finally presented in Sec. V.

II. MODEL EQUATIONS

The reduced fluid model investigated here is motivated by previous simulation studies performed by Sarazin *et al.*,^{69–71} Garcia *et al.*,^{72–74}, Myra *et al.*,^{75–77}, Bisai *et al.*,^{78–80} and Nielsen *et al.*^{81–83} One particular case of the model is equivalent to that used in Ref. 71 and simulates SOL conditions in the entire simulation domain where a particle source is located close to the

inner boundary. The particle density profile results from a balance between the plasma source, the sheath dissipation and radial transport due to the interchange instability. Another case of the model is similar to that used in Ref. 79 and features a simulation domain separating an edge region corresponding to plasma dynamics on closed magnetic flux surfaces and a SOL region where sheath dissipation balances the interchange drive. The source term is located in the plasma edge region where parallel resistivity gives rise to unstable drift waves. Despite these two fundamentally different descriptions of the primary instability mechanism underlying the SOL turbulence, the resulting fluctuations are remarkably similar as will be shown in the following.

We use two-field fluid model equations describing the plasma evolution in the edge and SOL regions for a quasi-neutral plasma, neglecting electron inertia and assuming for simplicity isothermal electrons and negligibly small ion temperature. We make these simplifying assumptions in order to obtain long fluctuation data time series from the numerical simulations. We choose a slab geometry where x refers to the radial direction and y to the binormal or poloidal direction. The reduced electron continuity and electron drift vorticity equations are given by

$$\frac{dn}{dt} + g \left(\frac{\partial n}{\partial y} - n \frac{\partial \phi}{\partial y} \right) = S_n + D_{\perp} \nabla_{\perp}^2 n + \left\langle \frac{1}{L_{\parallel}} \nabla_{\parallel} J_{\parallel e} \right\rangle_{\parallel}, \quad (1a)$$

$$\frac{d\nabla_{\perp}^2 \phi}{dt} + \frac{g}{n} \frac{\partial n}{\partial y} = v_{\perp} \nabla_{\perp}^4 \phi + \left\langle \frac{1}{nL_{\parallel}} \nabla_{\parallel} J_{\parallel} \right\rangle_{\parallel}, \quad (1b)$$

where n represents the normalized electron density, ϕ is the normalized electric potential, g is normalized effective gravity (that is, drive from unfavorable magnetic curvature), S_n is the plasma source term, and D_{\perp} and v_{\perp} are the normalized particle and vorticity diffusion coefficients. We use the standard Bohm normalization as previously used and discussed in Refs. 67–80. In addition we have the advective derivative $d/dt = \partial/\partial t + \mathbf{V}_E \cdot \nabla_{\perp}$, where $\mathbf{V}_E = \hat{\mathbf{z}} \times \nabla \phi$ is the electric drift. The plasma source term is given by $S_n(x) = S_0 \exp(-(x - x_0)^2/\lambda_s^2)$, where S_0 is the maximum amplitude of the source, x_0 is the source location and λ_s is the e -folding length for the source.

Equations (1) are averaged along the magnetic field lines, with the contribution from the normalized parallel electron $J_{\parallel e}$ and total plasma currents J_{\parallel} in the sheath connected regime given by

$$\left\langle \frac{1}{L_{\parallel}} \nabla_{\parallel} J_{\parallel e} \right\rangle_{\parallel} = -\sigma n \exp(\Lambda - \phi) + \chi(\hat{\phi} - \hat{n}), \quad (2a)$$

$$\left\langle \frac{1}{nL_{\parallel}} \nabla_{\parallel} J_{\parallel} \right\rangle_{\parallel} = \sigma [1 - \exp(\Lambda - \phi)] + \chi(\hat{\phi} - \hat{n}). \quad (2b)$$

Here Λ is the sheath potential, σ the normalized sheath dissipation and χ the normalized parallel plasma conductivity. Like in several previous investigations, these parameters are taken to be a function of the radial position in the boundary region.^{72–83} In particular, the sheath dissipation coefficient σ is finite in the SOL region ($x > x_{\text{SOL}}$) and vanishes in the edge ($x < x_{\text{SOL}}$), which corresponds to the region with closed magnetic flux surfaces,

$$\sigma(x) = \begin{cases} 0, & 0 \leq x < x_{\text{SOL}}, \\ \sigma_0, & x_{\text{SOL}} \leq x \leq L_x. \end{cases} \quad (3)$$

Similarly, the plasma conductivity χ is neglected in the SOL and is finite in the edge region,

$$\chi(x) = \begin{cases} \chi_0, & 0 \leq x < x_{\text{SOL}}, \\ 0, & x_{\text{SOL}} \leq x \leq L_x. \end{cases} \quad (4)$$

The simulation domain is sketched in Fig. 1, showing the location of the plasma source and the separation between the edge and SOL regions. Furthermore, the spatially fluctuating electron density \hat{n} and plasma potential $\hat{\phi}$ are defined as $\hat{n} = n - \langle n \rangle_y$ and $\hat{\phi} = \phi - \langle \phi \rangle_y$ where $\langle \cdot \rangle_y$ refers to the flux surface average. This leads to the final reduced electron continuity and electric drift vorticity equations,

$$\frac{dn}{dt} + g \left(\frac{\partial n}{\partial y} - n \frac{\partial \phi}{\partial y} \right) = S_n(x) + D_{\perp} \nabla_{\perp}^2 n - \sigma(x) n \exp(\Lambda - \phi) + \chi(x) (\hat{\phi} - \hat{n}), \quad (5a)$$

$$\frac{d\nabla_{\perp}^2 \phi}{dt} + \frac{g}{n} \frac{\partial n}{\partial y} = v_{\perp} \nabla_{\perp}^4 \phi + \sigma(x) [1 - \exp(\Lambda - \phi)] + \chi(x) (\hat{\phi} - \hat{n}). \quad (5b)$$

In the following we present results from numerical simulations of this model for two different cases. In the first case, the domain is split into two regions, effectively the edge and the SOL regions, by taking $x_{\text{SOL}} = 50$. In the second case, a pure SOL plasma is considered with $x_{\text{SOL}} = 0$, thus plasma conductivity χ is not present in the simulation domain.

The input parameters have been chosen to be similar to that used in previous publications based on this model.⁷⁹ For all runs presented here, the simulation domain lengths are chosen to be $L_x = 200$ and $L_y = 100$, with the border between the edge and the SOL at $x_{\text{SOL}} = 50$ for the two-region case. It has been verified that a change of the size of the simulation domain does not influence the fluctuation statistics. The simulation code is implemented in BOUT++⁸⁴ utilizing the STORM branch,⁸⁵ which uses a finite difference scheme in the x -direction and a spectral scheme in the y -direction. Time integration is performed with the PVODE solver.⁸⁶ We use a resolution

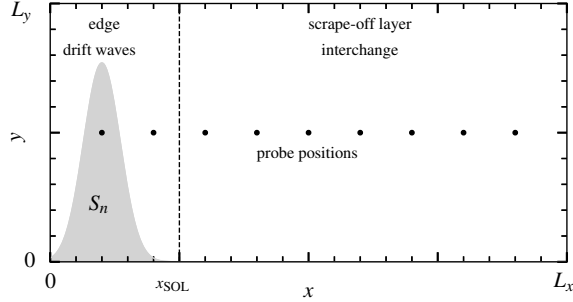


FIG. 1. Schematic illustration of the simulation domain for the $x_{\text{SOL}} = 50$ case. The position of the plasma source term (gray shaded) and the border between edge and SOL (dashed vertical line) are indicated.

of 512×256 grid points for all runs. We further take $D_{\perp} = \nu_{\perp} = 10^{-2}$, $g = 10^{-3}$, $\chi = 6 \times 10^{-4}$, $S_0 = 11/2000$, $\sigma_0 = 5 \times 10^{-4}$, $\Lambda = 0.5 \ln(2\pi m_i/m_e)$ with deuterium ions, $x_0 = 20$ and $\lambda_s = 10$. We apply periodic boundary conditions in the poloidal direction and zero gradient boundary conditions in the radial direction for both the electron density and vorticity fields. For the plasma potential we use zero gradient boundary conditions at the outer boundary and fixed boundary conditions $\phi(x=0) = 0$ at the inner boundary.

During the simulations, the plasma parameters at 9 different radial positions in the simulation domain are recorded with a sampling frequency of one in normalized time units. The location of these probes are presented in Fig. 1. This corresponds to single-point measurements in the experiments, and the simulation data will be analyzed in the same manner as has previously been done for experimental measurement data. The contour plots of the electron density in both simulation cases presented in Fig. 2 show several blob-like structures with the familiar mushroom-shape typical for strongly non-linear interchange motions.⁶⁵

Time series of the plasma parameters with a duration of 2×10^6 time units have been obtained under statistically stationary conditions, that is, excluding initial transients in the turbulence simulations. 10 simulation runs with this duration time are performed for the two-region model and 7 for the one region model. The fluctuation statistics to be presented in Sec. IV are based on these ensembles of simulation data. In the following analysis we will frequently consider plasma parameters normalized such as to have vanishing mean and unit standard deviation, for example. For the electron density we define

$$\tilde{n} = \frac{n - \langle n \rangle}{n_{\text{rms}}}, \quad (6)$$

where the angular brackets denote a time average and n_{rms} is the root mean square value calculated

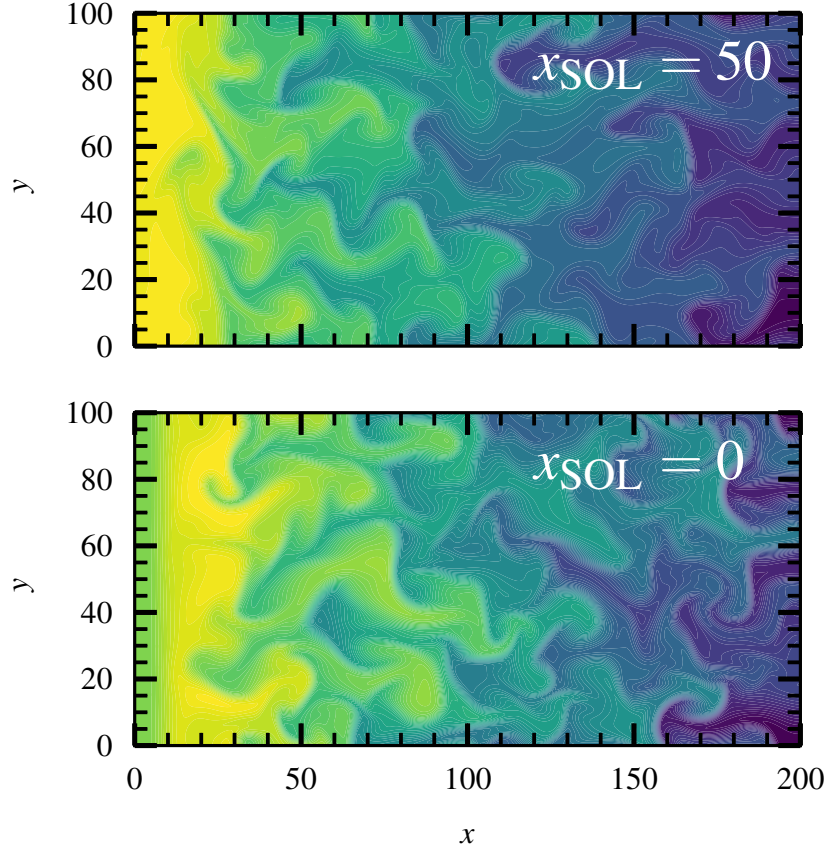


FIG. 2. Contour plots of $\log(n)$ in the turbulent state for the $x_{\text{SOL}} = 0$ and $x_{\text{SOL}} = 50$ cases showing the presence of mushroom-shaped blob-like structures in the SOL.

from the time series. A short part of the normalized electron density time series are presented in Fig. 3 for both simulation cases, showing frequent appearance of large-amplitude bursts due to the high density blob-like structures moving radially outwards. The radial variation of the lowest order moments of these fluctuations are presented and discussed in Sec. III.

In the following, the numerical simulation data will be compared to predictions of a stochastic model which describes the fluctuations as a super-position of uncorrelated pulses with fixed shape and constant duration. This is written as^{43–53}

$$\Psi_K(t) = \sum_{k=1}^{K(T)} A_k \psi\left(\frac{t-t_k}{\tau_d}\right), \quad (7)$$

where ψ is the pulse function, τ_d is the pulse duration time, $K(T)$ is the number of pulses for a realization of duration T , and for the event labelled k the pulse amplitude is A_k and the arrival

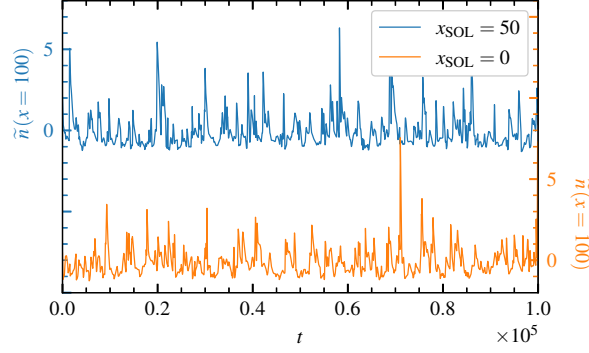


FIG. 3. A short part of the normalized electron density time series recorded at $x = 100$ for the $x_{\text{SOL}} = 0$ and $x_{\text{SOL}} = 50$ simulation cases.

time t_k . The mean value of the random variable Ψ_K is $\langle \Psi \rangle = (\tau_d / \tau_w) \langle A \rangle$, where $\langle A \rangle$ is the average pulse amplitude and τ_w is the average pulse waiting time. We will assume pulses arriving according to a Poisson process, which implies independent and exponentially distributed waiting times and independent arrival times uniformly distributed on the realization. We further assume independently and exponentially distributed amplitudes, $P_A(A) = \exp(-A/\langle A \rangle) / \langle A \rangle$, and we will consider the case of a two-sided exponential pulse function,⁵⁰

$$\psi(\theta; \lambda) = \begin{cases} \exp(\theta/\lambda), & \theta < 0, \\ \exp(-\theta/(1-\lambda)), & \theta \geq 0, \end{cases} \quad (8)$$

where the pulse asymmetry parameter λ is restricted to the range $0 < \lambda < 1$. For $\lambda < 1/2$, the pulse rise time is faster than the decay time, while the pulse shape is symmetric in the case $\lambda = 1/2$. The frequency power spectral density for this process is just the spectrum of the pulse function,⁵⁰

$$\Omega_{\tilde{\Psi}}(\omega) = \frac{2\tau_d}{[1 + (1-\lambda)^2(\tau_d\omega)^2][1 + \lambda^2(\tau_d\omega)^2]}, \quad (9)$$

where ω is the angular frequency. Note that the power spectral density of $\tilde{\Psi}$ is independent of the amplitude distribution. From this it follows that the frequency power spectral density can be used to estimate the pulse parameters τ_d and λ , which will be done in the following analysis of the numerical simulations.

The stationary probability density function (PDF) for the random variable Ψ_K can be shown to be a Gamma distribution,⁵³

$$\langle \Psi \rangle P_{\Psi}(\Psi) = \frac{\gamma}{\Gamma(\gamma)} \left(\frac{\gamma\Psi}{\langle \Psi \rangle} \right)^{\gamma-1} \exp\left(-\frac{\gamma\Psi}{\langle \Psi \rangle}\right), \quad (10)$$

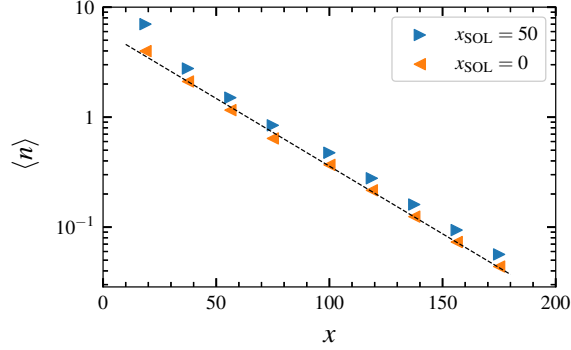


FIG. 4. Time-averaged electron density profile for the $x_{\text{SOL}} = 0$ and $x_{\text{SOL}} = 50$ cases. The broken line is the best fit of an exponential function with a scale length of 35.5.

with shape parameter $\gamma = \tau_d/\tau_w$, that is, the ratio of the pulse duration and the average pulse waiting time τ_w . This parameter describes the degree of pulse overlap, which determines the level of intermittency in the process. From the Gamma distribution it follows that the skewness moment is $S_\Psi = \langle(\Psi - \langle\Psi\rangle)^3\rangle/\Psi_{\text{rms}}^3 = 2/\gamma^{1/2}$ and the flatness moment is $F_\Psi = \langle(\Psi - \langle\Psi\rangle)^4\rangle/\Psi_{\text{rms}}^4 = 3 + 6/\gamma$. Accordingly, there is a parabolic relationship between these moments given by $F_\Psi = 3 + 3S_\Psi^2/2$. For strong pulse overlap and large γ , the probability density function approaches a normal distribution and the skewness S_Ψ and excess flatness $F_\Psi - 3$ moments vanish.

III. PROFILES AND DISTRIBUTIONS

The time-averaged electron density profiles in the turbulence simulations are presented in Fig. 4. Since the $x_{\text{SOL}} = 50$ case does not include any sheath dissipation in the edge region, the average density is higher here than for the $x_{\text{SOL}} = 0$ case. Throughout the entire SOL region, we observe that the electron density decreases exponentially with a radially constant scale length of 35.5. This is to be compared with the equilibrium SOL profile scale length in the absence of turbulence given by $(D_\perp/\sigma_0) = \sqrt{20}$ for the simulation parameters used here. Interestingly, both the scale length and the absolute density are very similar for the two simulation cases investigated. We further show the relative fluctuation level at different radial positions for both cases in Fig. 5. The normalized fluctuation level is very high, increases radially outwards and is roughly similar for the two simulation cases.

The radial variation of the skewness and flatness moments of the electron density fluctuations are presented in Figs. 6 and 7, respectively. From these figures it is clear that the intermittency of

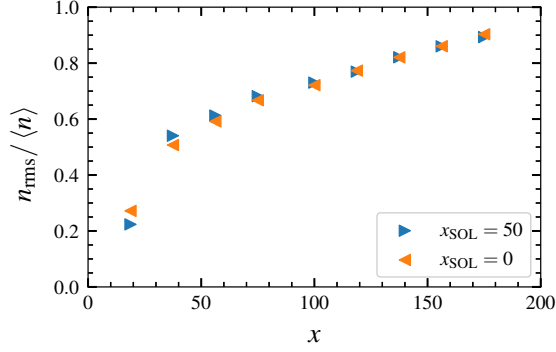


FIG. 5. The relative fluctuation level of the electron density at different positions in the SOL for the $x_{\text{SOL}} = 0$ and $x_{\text{SOL}} = 50$ cases.

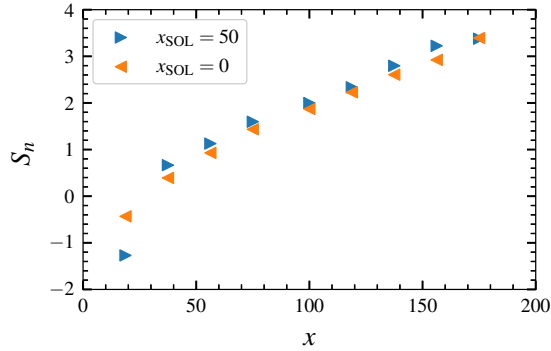


FIG. 6. Skewness of the electron density fluctuations at different radial positions for the $x_{\text{SOL}} = 0$ and $x_{\text{SOL}} = 50$ cases.

the fluctuations increases radially outwards in the SOL, qualitatively similar for the $x_{\text{SOL}} = 0$ and $x_{\text{SOL}} = 50$ cases. By plotting the flatness moment versus the skewness, presented in Fig. 8, it is seen that for both simulation cases there is a nearly parabolic relationship between these higher order moments. Such a parabolic relationship is predicted by the stochastic model describing the fluctuations as a super-position of uncorrelated pulses,^{43–46} which can be related to blob-like structures moving radially outwards in the SOL as seen in Fig. 2.

The PDFs for the normalized electron density fluctuations at different radial positions are presented in Figs. 9 and 10 for the $x_{\text{SOL}} = 0$ and $x_{\text{SOL}} = 50$ cases, respectively. The PDFs change from a narrow and nearly symmetric distribution in the edge/near SOL region to a distribution with an exponential tail for large fluctuation amplitudes in the far SOL. In Fig. 11 we further compare the PDFs of the electron density time series recorded in the far SOL at $x = 100$ for both simulation

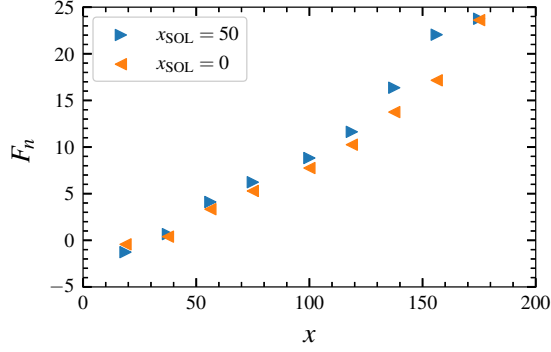


FIG. 7. Flatness of the electron density fluctuations at different radial positions for the $x_{\text{SOL}} = 0$ and $x_{\text{SOL}} = 50$ cases.

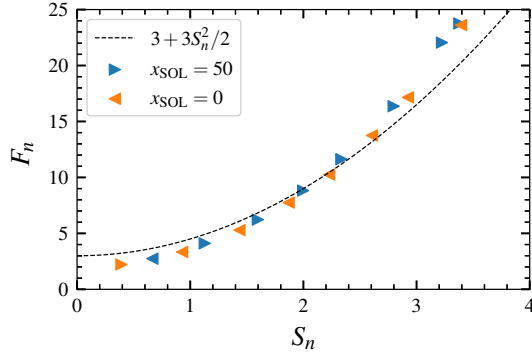


FIG. 8. Flatness plotted versus skewness for the electron density fluctuations in the SOL. The broken line shows the parabolic relationship $F_n = 3 + 3S_n^2/2$ for comparison.

cases with a Gamma distribution with a shape parameter of 1.4. Such a Gamma distribution is predicted by the stochastic model describing the fluctuations as a super-position of uncorrelated exponential pulses. The Gamma distribution is clearly an excellent description of the PDF for the electron density fluctuations in the simulations. A similar change in the shape of the PDF radially outwards in the SOL has also been reported from previous turbulence simulations.⁷²⁻⁷⁴

IV. FLUCTUATION STATISTICS

In this section we present a detailed analysis of the electron density fluctuations recorded at $x = 100$. In order to reveal the typical shape of large-amplitude bursts in the time series, a conditional averaging method which allows for overlapping events is applied. This identifies a total of 3128 conditional events with peak amplitudes larger than 2.5 times the root mean square value above

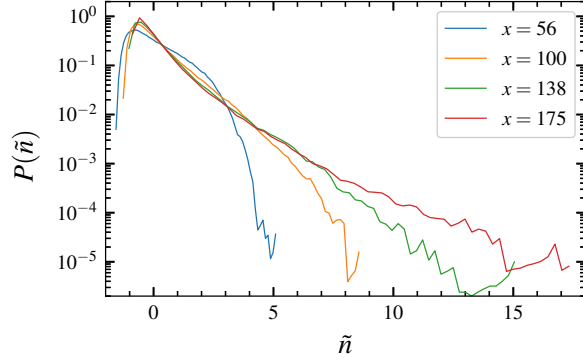


FIG. 9. Probability density functions of the normalized electron density recorded at different radial positions for the $x_{\text{SOL}} = 0$ case.

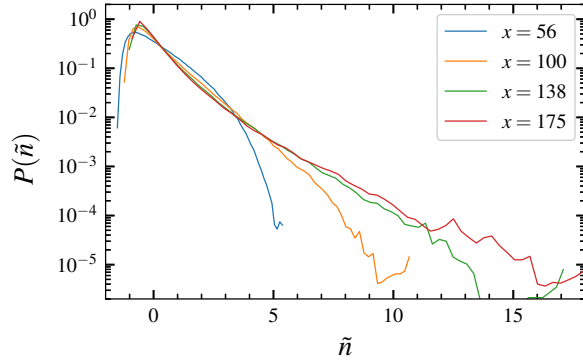


FIG. 10. Probability density functions of the normalized electron density recorded at different radial positions for the $x_{\text{SOL}} = 50$ case.

the mean for the $x_{\text{SOL}} = 50$ case and 1701 conditional events for the $x_{\text{SOL}} = 0$ case. The average burst structures are presented in Fig. 12 and shows an asymmetric shape with a fast rise and a slower decay. This is compared to an asymmetric, two-sided exponential function given by Eq. (8) with duration time $\tau_d = 300$ and asymmetry parameter $\lambda = 0.2$. The conditional burst shape is shown with semi-logarithmic axes in the inset in Fig. 12, showing that the decay of the conditional pulse shape is approximately exponential. However, the two-sided exponential function obviously fails to describe the smooth peak of the average burst shape in the simulations. As shown for short time lags in Fig. 12, this is better described using a skewed Lorentzian pulse as a fit function with duration 80 and skewness parameter 1 for the $x_{\text{SOL}} = 50$ case.^{87–90} The slightly elevated tails of the conditional burst shape is likely due to finite pulse overlap in the turbulence simulations.

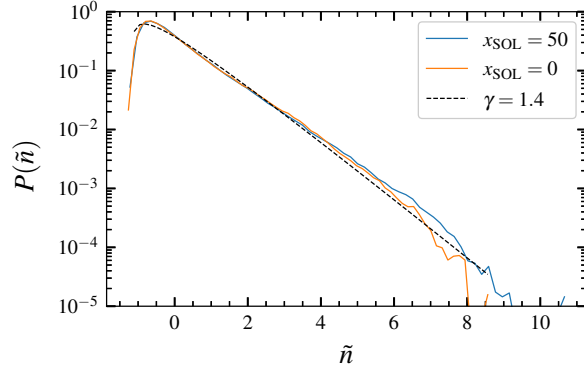


FIG. 11. Probability density functions of the normalized electron density recorded at $x = 100$ for both simulation cases compared to a Gamma distribution with shape parameter $\gamma = 1.4$ shown with the dashed black line.

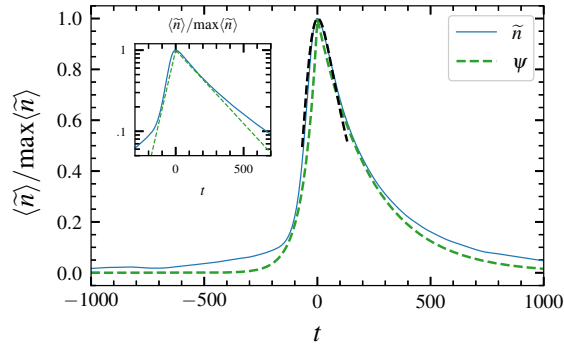


FIG. 12. Conditionally averaged burst shape at $x = 100$ of the $x_{\text{SOL}} = 50$ case (full blue line) compared to a two-sided exponential pulse (dashed orange line), as well as a skewed Lorentzian pulse for short time lags (dashed black line). The conditional average is normalized by its peak amplitude.

The frequency power spectral density of the electron density fluctuations recorded at $x = 100$ is presented with semi-logarithmic axes in Fig. 13 for the $x_{\text{SOL}} = 50$ case. This shows an exponential decrease of power with frequency for high frequencies. This exponential fall off is attributed to the smooth peak of the large-amplitude bursts in the simulations. In agreement with the fit of a Lorentzian function to the peak of the conditionally averaged burst shape in Fig. 12, the power spectral density decreases exponentially with a characteristic scale given by the duration of the Lorentzian-shaped peak.⁸⁹ The flattening of the power spectral density at low powers and high frequencies is due to the noise floor implied by round off errors in the computations.⁴⁹

The frequency power spectral density due to a super-position of uncorrelated exponential pulses

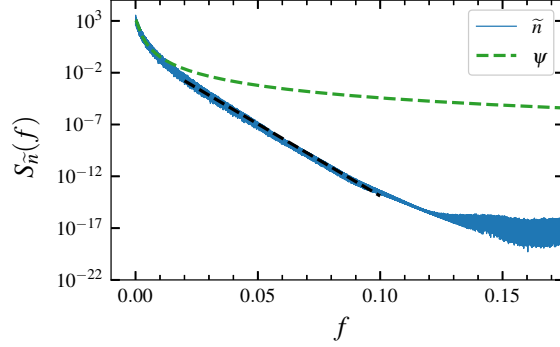


FIG. 13. Frequency power spectral density for the electron density fluctuations recorded at $x = 100$ for the $x_{\text{SOL}} = 50$ case (full line). This is compared to the predictions of a stochastic model describing the fluctuations as a super-position of uncorrelated, two-sided exponential pulses (dashed orange line), as well as an exponential function for the high frequency part (dashed black line).

is clearly not a good description of the simulation data for high frequencies. However, presenting the power spectrum with double-logarithmic axes shows that the spectrum given by Eq. (9) gives excellent agreement for high powers and low frequencies. This is clearly shown in Fig. 14 for the case $x_{\text{SOL}} = 50$. The exponential decay of the power at high frequencies is clearly due to the smooth peak of the large-amplitude bursts in the time series. This is consistent with the conditionally averaged burst shape presented in Fig. 12. Similar results for conditional averaging and frequency power spectra are found for the case $x_{\text{SOL}} = 0$ but with slightly different pulse parameters.

The conditionally averaged burst shape is presented in Fig. 15 for different radial positions in the SOL for the $x_{\text{SOL}} = 50$ case. Here it is seen that the burst shape in the far SOL region is the same for all radial positions, despite the fact that the relative fluctuation amplitude increases radially outwards. Accordingly, as predicted by the stochastic model, the frequency power spectral density has the same shape for all these different radial positions, as is shown in Figs. 16 and 17 for both the one- and two-region cases. The spectra are well described by that of a two-sided exponential pulse function, shown by the dashed black line in the figures.

Restricting the peak amplitude of conditional events in the electron density to be within a range of 2–4, 4–6 and 6–8 times the rms value, the appropriately scaled conditional burst shapes are presented in Fig. 18. This reveals that the average burst shape and duration do not depend on the burst amplitude and is again well described by a two-sided exponential function except for

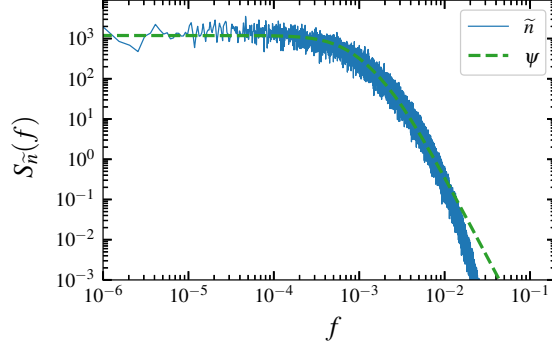


FIG. 14. Frequency power spectral density of the electron density fluctuations recorded at $x = 100$ for the $x_{\text{SOL}} = 50$ case (full blue line). This is compared to the predictions of a stochastic model describing the fluctuations as a super-position of uncorrelated, two-sided exponential pulses with duration time $\tau_d = 300$ and asymmetry parameter $\lambda = 0.2$ (dashed orange line).

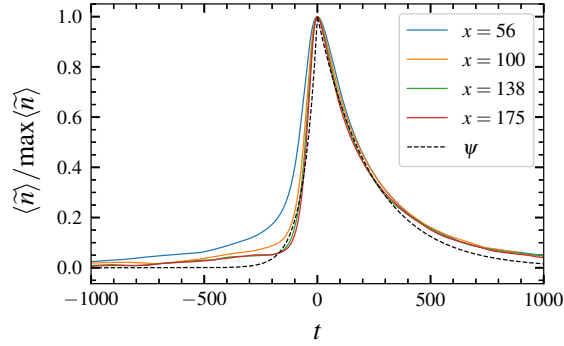


FIG. 15. Conditionally averaged burst shapes at different radial positions for the $x_{\text{SOL}} = 50$ case. The conditional averages are normalized by their peak amplitude.

the smooth peak. This supports the assumption of fixed pulse duration in the stochastic model describing the fluctuations as a super-positions of pulses.

From the conditional averaging we further obtain the peak amplitudes of conditional events and the waiting times between them. The PDFs of these are presented in Figs. 19 and 20, respectively. The distributions are similar for both simulation cases and are clearly well described by an exponential distribution as shown by the dashed black line in the plots. This is in agreement with the assumptions for the stochastic model presented in Sec. II. In particular, the exponential waiting time distribution supports the hypothesis that the events are uncorrelated and arrive according to a Poisson process.

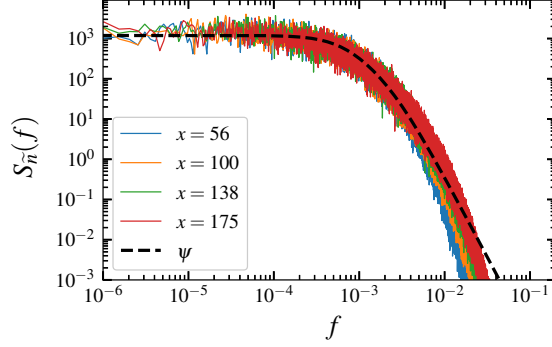


FIG. 16. Frequency power spectral densities of the electron density fluctuation recorded at different radial positions for the $x_{\text{SOL}} = 50$ model. The dashed line shows the spectrum due to a super-position of uncorrelated, two-sided exponential pulses with duration time τ_d .

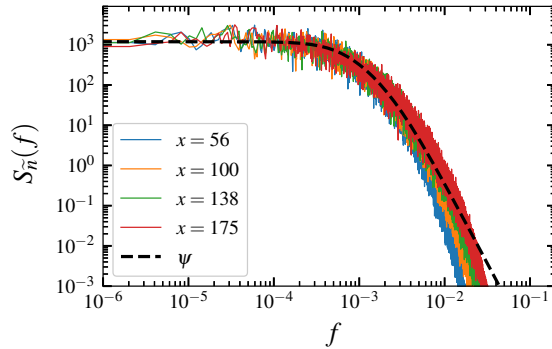


FIG. 17. Frequency power spectral densities of the electron density fluctuation recorded at different radial positions for the $x_{\text{SOL}} = 0$ model. The dashed line shows the spectrum due to a super-position of uncorrelated two-sided exponential pulses.

V. DISCUSSION AND CONCLUSIONS

The abundant experimental evidence for universal statistical properties of fluctuations in the SOL of magnetically confined fusion plasmas sets high requirements for validation of turbulence simulation codes for the boundary region.^{54–56} In this context, we have examined the statistical properties of the electron density fluctuations in the SOL by numerical simulations of plasma turbulence in the two-dimensional plane perpendicular to the magnetic field. Two model cases have been considered, one describing resistive drift waves in the edge region and another including only the interchange instability due to unfavorable magnetic field curvature. For both cases, mushroom-

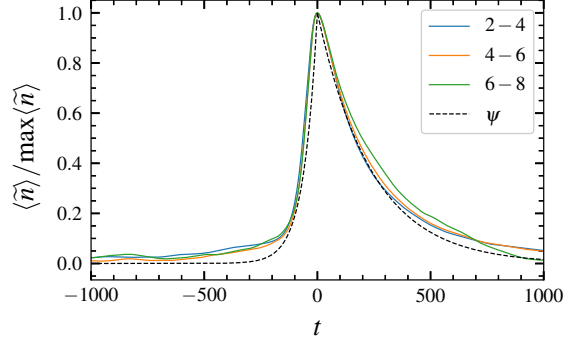


FIG. 18. Conditionally averaged burst shape at $x = 100$ of the $x_{\text{SOL}} = 50$ case for different conditional amplitude threshold intervals. The conditional averages are normalized by their peak amplitudes.

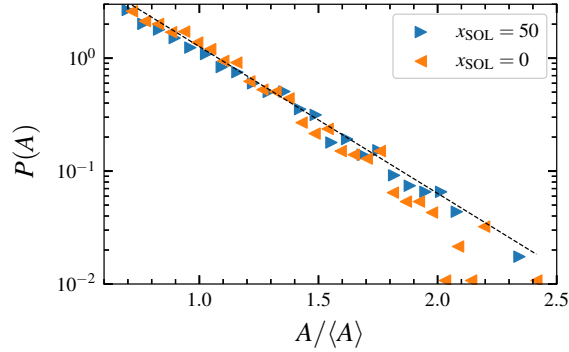


FIG. 19. Probability density functions of conditional burst amplitudes of the electron density time series recorded at $x = 100$.

shaped blob-like structures move radially outwards, resulting in large-amplitude fluctuations and high average particle densities in the SOL. The numerical simulations show that the time-averaged radial profile decreases exponentially with radial distance into the SOL with the same characteristic length scale for both simulation cases. Moreover, the fluctuation statistics in the SOL are the same for both cases. This is despite the different linear instability mechanisms driving the fluctuations in the edge/near SOL region in the two simulation cases. It appears that any drift-ordered instability mechanism will lead to formation of filament structures when coupled to a SOL region with unfavorable magnetic field curvature.

According to a stochastic model describing the profile as due to radial motion of filament structures, the profile scale length is given by the product of the radial filament velocity and the parallel transit time.^{46–48} This suggests that typical filament velocities are the same in both simulation

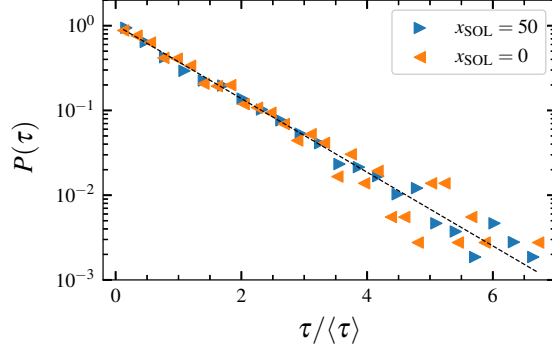


FIG. 20. Probability density functions of waiting times between consecutive large-amplitude burst in the electron density time series recorded at $x = 100$.

cases. Future work will investigate the distribution of filament sizes and velocities by analysis of the velocity fluctuations and applying a blob tracking algorithm as described in Ref. 91.

The relative fluctuation level increases radially outwards, nearly reaching unity in the far SOL for the plasma parameters investigated here. Similarly, the skewness and flatness moments also increase into the SOL, and these higher order moments closely follow a quadratic dependence as predicted by the stochastic model describing the fluctuations as a super-position of uncorrelated pulses. The PDF of the electron density fluctuations changes from a nearly Gaussian distribution in the edge/near SOL region to a distribution with an exponential tail for large amplitudes in the far SOL. In the far SOL region, the PDFs are well described by a Gamma distribution with the shape parameter given by the ratio of the pulse duration and average waiting time. The increase of this intermittency parameter with radial distance into the SOL suggests that only the most coherent and large-amplitude blob structures are able to move through the entire SOL region before they disperse and break up due to secondary instabilities.

A conditional averaging analysis has revealed that the shape of large-amplitude bursts in single-point recordings in the far SOL is well described by a two-sided exponential pulse, as has previously been found in experimental measurements. However, the high resolution and smoothness of the solution from the numerical computations implies that the burst structure has a rounded peak as opposed to the break point in experimental measurements due to their much lower sampling rate and additional measurement noise. The smooth peak is well described by a skewed Lorentzian pulse function. This is further supported by the frequency power spectral density, which is well described by that of a two-sided exponential pulse for high powers and low frequencies. However,

for low powers and high frequencies, the frequency power spectral density has an exponential decay which obviously can be attributed to the smooth, Lorentzian shaped peak of large-amplitude fluctuations in the numerical simulations. In experimental measurements, this exponential tail in the spectrum may readily be masked by low sampling rates, limiting the highest frequencies resolved, or by additive measurement noise, limiting the lowest power resolved.^{49,50}

In summary, it is here demonstrated that a simple but self-consistent model for turbulent fluctuations in the scrape-off layer reveals the same statistical properties of large-amplitude events as found in the experiments. This includes exponentially distributed pulse amplitudes and waiting times, the latter supporting the assumption of Poisson events.^{32,33,36,37,40,42} The simulation data also agree with predictions of the stochastic model, namely an exponential average profile, Gamma distributed fluctuation amplitudes and a frequency power spectral density determined by the average shape of large-amplitude bursts. It is concluded that the filtered Poisson process, describing the fluctuations in single-point recordings as a super-position of uncorrelated pulses with fixed duration, is an excellent description of the SOL plasma fluctuations in the turbulence simulations investigated here.

The simple turbulence model used in this study does not include finite ion temperature effects, X-point physics, parallel collisional conductivity in the scrape-off layer, or any effect of interactions with neutral particles. Numerous SOL turbulence models and codes are now being extended to include these features.^{92–100} The statistical framework with super-position of filaments can be used for analysis and interpretation of simulation results in these more advanced models, similar to what has been done here and previously for experimental measurements. As such, this work sets a new standard for validation of turbulence simulation codes.^{54–56}

ACKNOWLEDGEMENTS

This work was supported by the UiT Aurora Centre Program, UiT The Arctic University of Norway (2020). AT was supported by a Tromsø Science Foundation Starting Grant under grant number 19_SG_AT. GD acknowledges the generous hospitality of the Culham Centre for Fusion Energy (CCFE) where parts of this work were conducted. Two supercomputers provided by the Norwegian Metacenter for Computational Science (NOTUR) were used for the computational work, the Fram and Stallo clusters at the University of Tromsø under project nn9348k. The MARCONI supercomputer was used for parts of the computational work under the Project

No. FUA34_SOLBOUT4. The storm2d project has been used as a template for the presented physical models. This work was funded in part by the RCUK Energy Programme (Grant number EP/T012250/1) and the EPSRC Centre for Doctoral Training in the Science and Technology of Fusion Energy (Grant number EP/L01663X/1), as well as an iCASE award from CCFE.

DATA AVAILABILITY

The data that support the findings of this study are available from the corresponding author upon reasonable request.

REFERENCES

- ¹R. A. Pitts, J. P. Coad, D. P. Coster, G. Federici, W. Fundamenski, J. Horacek, K. Krieger, A. Kukushkin, J. Likonen, G. F. Matthews, M. Rubel, J. D. Strachan, and JET-EFDA contributors, “Material erosion and migration in tokamaks,” *Plasma Physics and Controlled Fusion* **47**, B303 (2005).
- ²B. Lipschultz, X. Bonnin, G. Counsell, A. Kallenbach, A. Kukushkin, K. Krieger, A. Leonard, A. Loarte, R. Neu, R. Pitts, T. Rognlien, J. Roth, C. Skinner, J. Terry, E. Tsitrone, D. Whyte, S. Zweben, N. Asakura, D. Coster, R. Doerner, R. Dux, G. Federici, M. Fenstermacher, W. Fundamenski, P. Ghendrih, A. Herrmann, J. Hu, S. Krasheninnikov, G. Kirnev, A. Kreter, V. Kurnaev, B. LaBombard, S. Lisgo, T. Nakano, N. Ohno, H. Pacher, J. Paley, Y. Pan, G. Pautasso, V. Philipps, V. Rohde, D. Rudakov, P. Stangeby, S. Takamura, T. Tanabe, Y. Yang, and S. Zhu, “Plasma–surface interaction, scrape-off layer and divertor physics: implications for ITER,” *Nuclear Fusion* **47**, 1189 (2007).
- ³A. Loarte, B. Lipschultz, A. Kukushkin, G. Matthews, P. Stangeby, N. Asakura, G. Counsell, G. Federici, A. Kallenbach, K. Krieger, A. Mahdavi, V. Philipps, D. Reiter, J. Roth, J. Strachan, D. Whyte, R. Doerner, T. Eich, W. Fundamenski, A. Herrmann, M. Fenstermacher, P. Ghendrih, M. Groth, A. Kirschner, S. Konoshima, B. LaBombard, P. Lang, A. Leonard, P. Monier-Garbet, R. Neu, H. Pacher, B. Pegourie, R. Pitts, S. Takamura, J. Terry, E. Tsitrone, and the ITPA Scrape-off Layer and Divertor Physics Topical Group, “Chapter 4: Power and particle control,” *Nuclear Fusion* **47**, S203 (2007).

- ⁴S. Wiesen, D. Reiter, V. Kotov, M. Baelmans, W. Dekeyser, A. S. Kukushkin, S. W. Lisgo, R. A. Pitts, V. Rozhansky, G. Saibene, I. Veselova, and S. Voskoboynikov, “The new SOLPS-ITER code package,” *Journal of Nuclear Materials* **463**, 480 (2015).
- ⁵X. Bonnin, W. Dekeyser, R. Pitts, D. Coster, S. Voskoboynikov, and S. Wiesen, “Presentation of the new SOLPS-ITER code package for tokamak plasma edge modelling,” *Plasma and Fusion Research* **11**, 1403102 (2016).
- ⁶D. A. D’Ippolito, J. R. Myra, S. I. Krasheninnikov, G. Q. Yu, and A. Y. Pigarov, “Blob transport in the tokamak scrape-off-layer,” *Contributions to Plasma Physics* **44**, 205 (2004).
- ⁷S. I. Krasheninnikov, D. A. D’Ippolito, and J. R. Myra, “Recent theoretical progress in understanding coherent structures in edge and SOL turbulence,” *Journal of Plasma Physics* **74**, 679 (2008).
- ⁸O. E. Garcia, “Blob transport in the plasma edge: a review,” *Plasma and Fusion Research* **4**, 019 (2009).
- ⁹D. A. D’Ippolito, J. R. Myra, and S. J. Zweben, “Convective transport by intermittent blob-filaments: Comparison of theory and experiment,” *Physics of Plasmas* **18**, 060501 (2011).
- ¹⁰N. Asakura, Y. Koide, K. Itami, N. Hosogan, K. Shimizu, S. Tsuji-Iio, S. Sakurai, and A. Sakasai, “SOI plasma profiles under radiative and detached divertor conditions in JT-60U,” *Journal of Nuclear Materials* **241-243**, 559 (1997).
- ¹¹B. LaBombard, R. L. Boivin, M. Greenwald, J. Hughes, B. Lipschultz, D. Mossessian, C. S. Pitcher, J. L. Terry, S. J. Zweben, and Alcator Group, “Particle transport in the scrape-off layer and its relationship to discharge density limit in Alcator C-Mod,” *Physics of Plasmas* **8**, 2107 (2001).
- ¹²B. Lipschultz, B. LaBombard, C. S. Pitcher, and R. Boivin, “Investigation of the origin of neutrals in the main chamber of Alcator C-Mod,” *Plasma Physics and Controlled Fusion* **44**, 733 (2002).
- ¹³O. E. Garcia, J. Horacek, R. A. Pitts, A. H. Nielsen, W. Fundamenski, J. P. Graves, V. Naulin, and J. J. Rasmussen, “Interchange turbulence in the TCV scrape-off layer,” *Plasma Physics and Controlled Fusion* **48**, L1 (2005).
- ¹⁴D. L. Rudakov, J. A. Boedo, R. A. Moyer, P. C. Stangeby, J. G. Watkins, D. G. Whyte, L. Zeng, N. H. Brooks, R. P. Doerner, T. E. Evans, M. E. Fenstermacher, M. Groth, E. M. Hollmann, S. I. Krasheninnikov, C. J. Lasnier, A. W. Leonard, M. A. Mahdavi, G. R. McKee, A. G. McLean, A. Y. Pigarov, W. R. Wampler, G. Wang, W. P. West, and C. P. C. Wong, “Far SOL transport

- and main wall plasma interaction in DIII-D,” *Nuclear Fusion* **45**, 1589 (2005).
- ¹⁵B. LaBombard, J. W. Hughes, D. Mossessian, M. Greenwald, B. Lipschultz, J. L. Terry, and the Alcator C-Mod Team, “Evidence for electromagnetic fluid drift turbulence controlling the edge plasma state in the Alcator C-Mod tokamak,” *Nuclear Fusion* **45**, 1658 (2005).
- ¹⁶O. E. Garcia, R. A. Pitts, J. Horacek, A. H. Nielsen, W. Fundamenski, V. Naulin, and J. J. Rasmussen, “Turbulent transport in the TCV SOL,” *Journal of Nuclear Materials* **363–365**, 575 (2007).
- ¹⁷O. E. Garcia, J. Horacek, R. A. Pitts, A. H. Nielsen, W. Fundamenski, V. Naulin, and J. J. Rasmussen, “Fluctuations and transport in the TCV scrape-off layer,” *Nuclear Fusion* **47**, 667 (2007).
- ¹⁸O. E. Garcia, R. A. Pitts, J. Horacek, J. Madsen, V. Naulin, A. H. Nielsen, and J. J. Rasmussen, “Collisionality dependent transport in TCV SOL plasmas,” *Plasma Physics and Controlled Fusion* **49**, B47 (2007).
- ¹⁹D. Carralero, G. Birkenmeier, H. W. Müller, P. Manz, P. deMarne, S. H. Müller, F. Reimold, U. Stroth, M. Wischmeier, E. Wolfrum, and The ASDEX Upgrade Team, “An experimental investigation of the high density transition of the scrape-off layer transport in ASDEX Upgrade,” *Nuclear Fusion* **54**, 123005 (2014).
- ²⁰D. Carralero, H. W. Müller, M. Groth, M. Komm, J. Adamek, G. Birkenmeier, M. Brix, F. Janky, P. Hacek, S. Marsen, F. Reimold, C. Silva, U. Stroth, M. Wischmeier, E. Wolfrum, ASDEX Upgrade Team, COMPASS Team, and JET-EFDA Contributors, “Implications of high density operation on sol transport: A multimachine investigation,” *Journal of Nuclear Materials* **463**, 123 (2015).
- ²¹F. Militello, L. Garzotti, J. Harrison, J. T. Omotani, R. Scannell, S. Allan, A. Kirk, I. Lupelli, A. J. Thornton, and the MAST team, “Characterisation of the L-mode scrape off layer in MAST: decay lengths,” *Nuclear Fusion* **56**, 016006 (2016).
- ²²N. Vianello, C. Tsui, C. Theiler, S. Allan, J. Boedo, B. Labit, H. Reimerdes, K. Verhaegh, W. A. J. Vijvers, N. Walkden, S. Costea, J. Kovacic, C. Ionita, V. Naulin, A. H. Nielsen, J. J. Rasmussen, B. Schneider, R. Schrittwieser, M. Spolaore, D. Carralero, J. Madsen, B. Lipschultz, F. Militello, The TCV Team, and The EUROfusion MST1 Team, “Modification of SOL profiles and fluctuations with line-average density and divertor flux expansion in TCV,” *Nuclear Fusion* **57**, 116014 (2017).

- ²³N. Vianello, D. Carralero, C. K. Tsui, V. Naulin, M. Agostini, I. Cziegler, B. Labit, C. Theiler, E. Wolfrum, D. Aguiam, S. Allan, M. Bernert, J. Boedo, S. Costea, H. De Oliveira, O. Fevrier, J. Galdon-Quiroga¹, G. Grenfell, A. Hakola, C. Ionita, H. Isliker, A. Karpushov, J. Kovacic, B. Lipschultz, R. Maurizio, K. McClements, F. Militello, A. H. Nielsen, J. Olsen, J. J. Rasmussen, T. Ravensbergen, H. Reimerdes, B. Schneider, R. Schrittwieser, E. Seliunin, M. Spolaore, K. Verhaegh, J. Vicente, N. Walkden, W. Zhang, the ASDEX Upgrade Team, the TCV Team, and the EUROfusion MST1 Team, “Scrape-off layer transport and filament characteristics in high-density tokamak regimes,” *Nuclear Fusion* **60**, 016001 (2020).
- ²⁴P. C. Liewer, “Measurements of microturbulence in tokamaks and comparisons with theories of turbulence and anomalous transport,” *Nuclear Fusion* **25**, 543 (1985).
- ²⁵M. Endler, “Turbulent SOL transport in stellarators and tokamaks,” *Journal of Nuclear Materials* **266-269**, 84 (1999).
- ²⁶B. A. Carreras, “Plasma edge cross-field transport: experiment and theory,” *Journal of Nuclear Materials* **337**, 315 (2005).
- ²⁷S. J. Zweben, J. A. Boedo, O. Grulke, C. Hidalgo, B. LaBombard, R. J. Maqueda, P. Scarin, and J. L. Terry, “Edge turbulence measurements in toroidal fusion devices,” *Plasma Physics and Controlled Fusion* **49**, S1 (2007).
- ²⁸O. E. Garcia, I. Cziegler, R. Kube, B. LaBombard, and J. L. Terry, “Burst statistics in Alcator C-Mod SOL turbulence,” *Journal of Nuclear Materials* **438**, S180 (2013).
- ²⁹O. E. Garcia, S. M. Fritzner, R. Kube, I. Cziegler, B. LaBombard, and J. L. Terry, “Intermittent fluctuations in the Alcator C-Mod scrape-off layer,” *Physics of Plasmas* **20**, 055901 (2013).
- ³⁰O. E. Garcia, J. Horacek, and R. A. Pitts, “Intermittent fluctuations in the TCV scrape-off layer,” *Nuclear Fusion* **55**, 062002 (2015).
- ³¹A. Theodorsen, O. E. Garcia, J. Horacek, R. Kube, and R. A. Pitts, “Scrape-off layer turbulence in TCV: Evidence in support of stochastic modelling,” *Plasma Physics and Controlled Fusion* **58**, 044006 (2016).
- ³²O. E. Garcia, R. Kube, A. Theodorsen, J.-G. Bak, S.-H. Hong, H.-S. Kim, R. A. Pitts, and KSTAR Team, “SOL width and intermittent fluctuations in KSTAR,” *Nuclear Materials and Energy* **12**, 36 (2017).
- ³³A. Theodorsen, O. E. Garcia, R. Kube, B. LaBombard, and J. L. Terry, “Relationship between frequency power spectra and intermittent, large-amplitude bursts in the Alcator C-Mod scrape-off layer,” *Nuclear Fusion* **57**, 114004 (2017).

- ³⁴N. R. Walkden, A. Wynn, F. Militello, B. Lipschultz, G. Matthews, C. Guillemaut, J. Harrison, D. Moulton, and JET Contributors, “Statistical analysis of the ion flux to the JET outer wall,” *Nuclear Fusion* **57**, 036016 (2017).
- ³⁵N. R. Walkden, A. Wynn, F. Militello, B. Lipschultz, G. Matthews, C. Guillemaut, J. Harrison, D. Moulton, and J. Contributors, “Interpretation of scrape-off layer profile evolution and first-wall ion flux statistics on JET using a stochastic framework based on filamentary motion,” *Plasma Physics and Controlled Fusion* **59**, 085009 (2017).
- ³⁶R. Kube, O. E. Garcia, A. Theodorsen, D. Brunner, A. Q. Kuang, B. LaBombard, and J. L. Terry, “Intermittent electron density and temperature fluctuations and associated fluxes in the Alcator C-Mod scrape-off layer,” *Plasma Physics and Controlled Fusion* **60**, 065002 (2018).
- ³⁷O. E. Garcia, R. Kube, A. Theodorsen, B. LaBombard, and J. L. Terry, “Intermittent fluctuations in the Alcator C-Mod scrape-off layer for ohmic and high confinement mode plasmas,” *Physics of Plasmas* **25**, 056103 (2018).
- ³⁸A. Theodorsen, O. E. Garcia, R. Kube, B. LaBombard, and J. L. Terry, “Universality of Poisson-driven plasma fluctuations in the Alcator C-Mod scrape-off layer,” *Physics of Plasmas* **25**, 122309 (2018).
- ³⁹A. Bencze, M. Berta, A. Buzás, P. Hacek, J. Krbec, M. Szutyányi, and the COMPASS Team, “Characterization of edge and scrape-off layer fluctuations using the fast Li-BES system on compass,” *Plasma Physics and Controlled Fusion* **61**, 085014 (2019).
- ⁴⁰R. Kube, O. E. Garcia, A. Theodorsen, A. Q. Kuang, B. LaBombard, J. L. Terry, and D. Brunner, “Statistical properties of the plasma fluctuations and turbulent cross-field fluxes in the outboard mid-plane scrape-off layer of Alcator C-Mod,” *Nuclear Materials and Energy* **18**, 193 (2019).
- ⁴¹A. Kuang, B. LaBombard, D. Brunner, O. E. Garcia, R. Kube, and A. Theodorsen, “Plasma fluctuations in the scrape-off layer and at the divertor target in Alcator C-Mod and their relationship to divertor collisionality and density shoulder formation,” *Nuclear Materials and Energy* **19**, 295 (2019).
- ⁴²R. Kube, A. Theodorsen, O. E. Garcia, D. Brunner, B. LaBombard, and J. L. Terry, “Comparison between mirror Langmuir probe and gas-puff imaging measurements of intermittent fluctuations in the Alcator C-Mod scrape-off layer,” *Journal of Plasma Physics* **86**, 905860519 (2020).

- ⁴³O. E. Garcia, “Stochastic modeling of intermittent scrape-off layer plasma fluctuations,” *Physical Review Letters* **108**, 265001 (2012).
- ⁴⁴R. Kube and O. E. Garcia, “Convergence of statistical moments of particle density time series in scrape-off layer plasmas,” *Physics of Plasmas* **22**, 012502 (2015).
- ⁴⁵A. Theodorsen and O. E. Garcia, “Level crossings, excess times, and transient plasma–wall interactions in fusion plasmas,” *Physics of Plasmas* **23**, 040702 (2016).
- ⁴⁶O. E. Garcia, R. Kube, A. Theodorsen, and H. L. Pécseli, “Stochastic modelling of intermittent fluctuations in the scrape-off layer: Correlations, distributions, level crossings, and moment estimation,” *Physics of Plasmas* **23**, 052308 (2016).
- ⁴⁷F. Militello and J. T. Omotani, “Scrape off layer profiles interpreted with filament dynamics,” *Nuclear Fusion* **56**, 104004 (2016).
- ⁴⁸F. Militello and J. T. Omotani, “On the relation between non-exponential scrape off layer profiles and the dynamics of filaments,” *Nuclear Fusion* **58**, 125004 (2016).
- ⁴⁹A. Theodorsen and O. E. Garcia, “Statistical properties of a filtered Poisson process with additive random noise: distributions, correlations and moment estimation,” *Physica Scripta* **92**, 054002 (2017).
- ⁵⁰O. E. Garcia and A. Theodorsen, “Auto-correlation function and frequency spectrum due to a super-position of uncorrelated exponential pulses,” *Physics of Plasmas* **24**, 032309 (2017).
- ⁵¹A. Theodorsen and O. E. Garcia, “Level crossings and excess times due to a superposition of uncorrelated exponential pulses,” *Physical Review E* **97**, 012110 (2018).
- ⁵²F. Militello, T. Farley, K. Mukhi, N. Walkden, and J. T. Omotani, “A two-dimensional statistical framework connecting thermodynamic profiles with filaments in the scrape off layer and application to experiments,” *Physics of Plasmas* **25**, 056112 (2018).
- ⁵³A. Theodorsen and O. E. Garcia, “Probability distribution functions for intermittent scrape-off layer plasma fluctuations,” *Plasma Physics and Controlled Fusion* **60**, 034006 (2018).
- ⁵⁴P. W. Terry, M. Greenwald, J.-N. Leboeuf, G. R. McKee, D. R. Mikkelsen, W. M. Nevins, D. E. Newman, D. P. Stotler, Task Group on Verification and Validation, U.S. Burning Plasma Organization, and U.S. Transport Task Force, “Validation in fusion research: Towards guidelines and best practices,” *Physics of Plasmas* **15**, 062503 (2008).
- ⁵⁵M. Greenwald, “Verification and validation for magnetic fusion,” *Plasma Physics and Controlled Fusion* **17**, 058101 (2010).

- ⁵⁶C. Holland, “Validation metrics for turbulent plasma transport,” *Physics of Plasmas* **23**, 060901 (2016).
- ⁵⁷G. Decristoforo, A. Theodorsen, and O. E. Garcia, “Intermittent fluctuations due to Lorentzian pulses in turbulent thermal convection,” *Physics of Fluids* **32**, 085102 (2020).
- ⁵⁸O. Pogutse, W. Kerner, V. Gribkov, S. Bazdenkov, and M. Osipenko, “The resistive interchange convection in the edge of tokamak plasmas,” *Plasma Physics and Controlled Fusion* **36**, 1963 (1994).
- ⁵⁹H. Sugama and W. Horton, “L-H confinement mode dynamics in three-dimensional state space,” *Plasma Physics and Controlled Fusion* **37**, 345 (1995).
- ⁶⁰P. Beyer and K. H. Spatschek, “Center manifold theory for the dynamics of the L–H-transition,” *Physics of Plasmas* **3**, 995 (1996).
- ⁶¹W. Horton, G. Hu, and G. Laval, “Turbulent transport in mixed states of convective cells and sheared flows,” *Physics of Plasmas* **3**, 2912 (1996).
- ⁶²M. Berning and K. H. Spatschek, “Bifurcations and transport barriers in the resistive-g paradigm,” *Physical Review E* **62**, 1162 (2000).
- ⁶³O. E. Garcia, N. H. Bian, J.-V. Paulsen, S. Benkadda, and K. Rypdal, “Confinement and bursty transport in a flux-driven convection model with sheared flows,” *Plasma Physics and Controlled Fusion* **45**, 919 (2003).
- ⁶⁴O. E. Garcia and N. H. Bian, “Bursting and large-scale intermittency in turbulent convection with differential rotation,” *Physical Review E* **68**, 047301 (2003).
- ⁶⁵O. E. Garcia, N. H. Bian, V. Naulin, A. H. Nielsen, and J. J. Rasmussen, “Two-dimensional convection and interchange motions in fluids and magnetized plasmas,” *Physica Scripta* **T122**, 104 (2003).
- ⁶⁶F. Wilczynski, D. W. Hughes, S. V. Loo, W. Arter, and F. Militello, “Stability of scrape-off layer plasma: A modified Rayleigh–Bénard problem,” *Physics of Plasmas* **26**, 022510 (2019).
- ⁶⁷S. Benkadda, X. Garbet, and A. Verma, “Interchange instability turbulence model in edge tokamak plasma,” *Contributions to Plasma Physics* **34**, 247 (1994).
- ⁶⁸O. E. Garcia, “Two-field transport models for magnetized plasmas,” *Journal of Plasma Physics* **65**, 81 (2001).
- ⁶⁹Y. Sarazin and P. Ghendrih, “Intermittent particle transport in two-dimensional edge turbulence,” *Physics of Plasmas* **5**, 4214 (1998).

- ⁷⁰P. Ghendrih, Y. Sarazin, G. Attuel, S. Benkadda, P. Beyer, G. Falchetto, C. Figarella, X. Garbet, V. Grandgirard, and M. Ottaviani, “Theoretical analysis of the influence of external biasing on long range turbulent transport in the scrape-off layer,” *Nuclear Fusion* **43**, 1013 (2003).
- ⁷¹Y. Sarazin, P. Ghendrih, G. Attuel, C. Clément, X. Garbet, V. Grandgirard, M. Ottaviani, S. Benkadda, P. Beyer, N. Bian, and C. Figarella, “Theoretical understanding of turbulent transport in the SOL,” *Journal of Nuclear Materials* **313**, 796 (2003).
- ⁷²O. E. Garcia, V. Naulin, A. H. Nielsen, and J. J. Rasmussen, “Computations of intermittent transport in scrape-off layer plasmas,” *Physical Review Letters* **92**, 165003 (2004).
- ⁷³O. E. Garcia, V. Naulin, A. H. Nielsen, and J. J. Rasmussen, “Turbulence and intermittent transport at the boundary of magnetized plasmas,” *Physics of Plasmas* **12**, 062309 (2005).
- ⁷⁴O. E. Garcia, V. Naulin, A. H. Nielsen, and J. J. Rasmussen, “Turbulence simulations of blob formation and radial propagation in toroidally magnetized plasmas,” *Physica Scripta* **T122**, 89 (2006).
- ⁷⁵J. R. Myra, D. A. Russell, and D. A. D’Ippolito, “Transport of perpendicular edge momentum by drift-interchange turbulence and blobs,” *Physics of Plasmas* **15**, 032304 (2008).
- ⁷⁶D. A. Russell, J. R. Myra, and D. A. D’Ippolito, “Saturation mechanisms for edge turbulence,” *Physics of Plasmas* **16**, 122304 (2009).
- ⁷⁷J. R. Myra, W. M. Davis, D. A. D’Ippolito, B. LaBombard, D. A. Russell, J. L. Terry, and S. J. Zweben, “Edge sheared flows and the dynamics of blob-filaments,” *Nuclear Fusion* **53**, 073013 (2013).
- ⁷⁸N. Bisai, A. Das, S. Deshpande, R. Jha, P. Kaw, A. Sen, and R. Singh, “Simulation of plasma transport by coherent structures in scrape-off-layer tokamak plasmas,” *Physics of Plasmas* **11**, 4018 (2004).
- ⁷⁹N. Bisai, A. Das, S. Deshpande, R. Jha, P. Kaw, A. Sen, and R. Singh, “Edge and scrape-off layer tokamak plasma turbulence simulation using two-field fluid model,” *Physics of Plasmas* **12**, 072520 (2005).
- ⁸⁰N. Bisai, A. Das, S. Deshpande, R. Jha, P. Kaw, A. Sen, and R. Singh, “Formation of a density blob and its dynamics in the edge and the scrape-off layer of a tokamak plasma,” *Physics of Plasmas* **12**, 102515 (2005).
- ⁸¹A. H. Nielsen, G. S. Xu, J. Madsen, V. Naulin, J. J. Rasmussen, and B. N. Wan, “Simulation of transition dynamics to high confinement in fusion plasmas,” *Physics Letters A* **379**, 3097 (2015).

- ⁸²A. H. Nielsen, J. J. Rasmussen, J. Madsen, G. S. Xu, V. Naulin, J. M. B. Olsen, M. Løiten, S. K. Hansen, N. Yan, L. Tophøj, and B. N. Wan, “Numerical simulations of blobs with ion dynamics,” *Plasma Physics and Controlled Fusion* **59**, 025012 (2017).
- ⁸³J. Olsen, A. H. Nielsen, J. J. Rasmussen, J. Madsen, T. Eich, B. Sieglin, and V. Naulin, “Scrape-off layer power fall-off length from turbulence simulations of ASDEX Upgrade L-mode,” *Plasma Physics and Controlled Fusion* **60**, 085018 (2018).
- ⁸⁴B. Dudson, M. Umansky, X. Xu, P. Snyder, and H. Wilson, “BOUT++: A framework for parallel plasma fluid simulations,” *Computer Physics Communications* **180**, 1467 (2009).
- ⁸⁵F. Militello, B. Dudson, L. Easy, A. Kirk, and P. Naylor, “On the interaction of scrape off layer filaments,” *Plasma Physics and Controlled Fusion* **59**, 125013 (2017).
- ⁸⁶G. D. Byrne and A. C. Hindmarsh, “PVODE, an ODE solver for parallel computers,” *The International Journal of High Performance Computing Applications* **13**, 354 (1999).
- ⁸⁷J. E. Maggs and G. J. Morales, “Generality of deterministic chaos, exponential spectra, and Lorentzian pulses in magnetically confined plasmas,” *Physical Review Letters* **107**, 185003 (2011).
- ⁸⁸O. E. Garcia and A. Theodorsen, “Power law spectra and intermittent fluctuations due to uncorrelated Lorentzian pulses,” *Physics of Plasmas* **24**, 020704 (2017).
- ⁸⁹O. E. Garcia and A. Theodorsen, “Skewed Lorentzian pulses and exponential frequency power spectra,” *Physics of Plasmas* **25**, 014503 (2018).
- ⁹⁰O. E. Garcia and A. Theodorsen, “Intermittent fluctuations due to uncorrelated Lorentzian pulses,” *Physics of Plasmas* **25**, 014506 (2018).
- ⁹¹G. Decristoforo, F. Militello, T. Nicholas, J. Omotani, C. Marsden, N. Walkden, and O. E. Garcia, “Blob interactions in 2D scrape-off layer simulations,” *Physics of Plasmas* **27**, 122301 (2020).
- ⁹²F. D. Halpern, P. Ricci, S. Jolliet, J. Loizu, J. Morales, A. Masetto, F. Musil, F. Riva, T. M. Tran, and C. Wersal, “The GBS code for tokamak scrape-off layer simulations,” *Journal of Computational Physics* **315**, 388 (2016).
- ⁹³P. Tamain, H. Bufferand, G. Ciraoloa, C. Colin, D. Galassi, P. Ghendrih, and F. Schwander, “The TOKAM3X code for edge turbulence fluid simulations of tokamak plasmas in versatile magnetic geometries,” *Journal of Computational Physics* **321**, 606 (2016).
- ⁹⁴B. D. Dudson and J. Leddy, “Hermes: global plasma edge fluid turbulence simulations,” *Plasma Physics and Controlled Fusion* **59**, 054010 (2017).

- ⁹⁵M. Held, M. Wiesenberger, R. Kube, and A. Kendl, “Non-Oberbeck–Boussinesq zonal flow generation,” *Nuclear Fusion* **58**, 104001 (2018).
- ⁹⁶M. Wiesenberger, L. Einkemmer, M. Held, A. Gutierrez-Milla, X. Sáez, and R. Iakymchuk, “Reproducibility, accuracy and performance of the FELTOR code and library on parallel computer architectures,” *Computer Physics Communications* **238**, 145 (2019).
- ⁹⁷A. Stegmeir, A. Ross, T. Body, M. Francisquez, W. Zholobenko, D. Coster, F. Jenko, B. N. Rogers, and K. S. Kang, “Global turbulence simulations of the tokamak edge region with GRILLIX,” *Physics of Plasmas* **26**, 052517 (2019).
- ⁹⁸D. R. Zhang, Y. P. Chen, X. Q. Xu, and T. Y. Xia, “Self-consistent simulation of transport and turbulence in tokamak edge plasma by coupling SOLPS-ITER and BOUT++,” *Physics of Plasmas* **26**, 012508 (2019).
- ⁹⁹D. A. Russell, J. R. Myra, and D. P. Stotler, “A reduced model of neutral-plasma interactions in the edge and scrape-off-layer: Verification comparisons with kinetic Monte Carlo simulations,” *Physics of Plasmas* **26**, 022304 (2019).
- ¹⁰⁰M. Giacomini and P. Ricci, “Investigation of turbulent transport regimes in the tokamak edge by using two-fluid simulations,” *Journal of Plasma Physics* **86**, 905860502 (2020).